

Performance improvement for ADCPs on surface buoys

David W. Velasco
Nortek Group
Boston, USA

david.velasco@nortekgroup.com

Sven Nylund
Nortek Group
Oslo, Norway

Abstract— Improvements to motion compensation in current profile data from surface buoys have been previously presented [1] and here we expand on this previous work on the integration of Attitude and Heading Reference Sensors (AHRS) to Acoustic Doppler Current Profilers (ADCP). Presently, the applicability of surface buoy-mounted ADCPs is generally limited to those applications where spatial and temporal averaging are acceptable methods to address motion concerns. However, the increasing demand from both the research and operational communities for ever finer resolution in space and time is rendering averaging as an unacceptable method for these type of deployments. But recent technological advances in miniature gyro-compensated motion sensors (improved accuracy and resolution, and reduction in physical size, power consumption, and cost) addresses some of the earlier concerns with surface buoy-mounted ADCPs. This is achieved through real-time bin mapping at the individual ping level where true tilt data is derived from the AHRS, as opposed to non-gyro-compensated tilt sensors that are the norm for ADCPs up to now. These advances allow for more precise validation of surface buoy-mounted ADCP data against static-mounted reference systems. Data from test deployments is presented, including comparison with reference systems, as well as comparison with simulated “standard” tilt sensors.

Keywords— ADCP, surface buoy, currents, AHRS, bin mapping

I. INTRODUCTION

The benefits of mounting ADCPs in surface buoys have been readily recognized [2-7]. These include: easier access for maintenance, simpler infrastructure required to send real-time data to telemetry systems on the buoy, and ability to measure long time-series of near surface currents and current profiling from a single instrument. However, some authors have discussed how surface buoy-mounted ADCPs also suffered from issues not generally faced when deployed on bottom frames or more stable subsurface buoys [8-10], including: wave-induced vertical velocities, rapid instrument rotation rates, dynamic attitude variations, interference from near surface bubbles, velocity bias due to plankton migration and pelagic fish interference.

As ADCP technology grew in acceptance within the oceanographic community, several studies were carried out to validate current profile data collected from surface buoys. These were mostly done through comparisons with reference systems (such as Vector-Measuring Current Meters or bottom-mounted ADCPs) as well as against theoretical values [11-18]. In general these studies report agreeable comparisons. However, due mostly to lack of surface buoy motion measurement and compensation, they almost exclusively focused on large spatial

and temporal scales. So while some of the previously mentioned issues were dealt with by averaging in space and time, the technology available has been insufficient to address all concerns, especially for studies requiring finer spatial and temporal resolutions, as is more the case nowadays.

With this in mind, three separate experiments have been conducted within the Chesapeake Bay, USA in 2014, 2016 and 2018 [19-22, 1], each with progressive levels of success in understanding the impact of buoy motion on ADCP velocity profile data. They have shown that the lack of buoy motion measurement and compensation, coupled with inadequate bin mapping, leads to inaccuracies between surface buoy-mounted ADCPs and collocated reference systems, in particular when the ADCP is to be mounted on smaller (under 2 m diameter) wave following buoy platforms. This is especially the case during times of strong vertical shear and large buoy angular velocity. The last of these three experiments [1] showed direct evidence of velocity accuracy improvements by using a state-of-the-art ADCP with an embedded AHRS. This allowed for real-time bin mapping on a ping-by-ping basis by using true tilt from a gyro-compensated motion sensor. The present work expands these previous experiences, in particular the last experiment, to better describe and quantify the improvements gained. For simplicity, here we only consider vertically-mounted ADCPs; that is, either bottom-mounted, up-looking, or, surface-mounted, down-looking systems.

II. METHOD DESCRIPTION

A. Basic ADCP Processing Considerations

In order to build a velocity profile in Earth coordinates, ADCPs go through a three-step process. First, radial (“BEAM”) velocities are measured within time-gated intervals (depth bins) defined along each beam. Second, the radial velocities are converted to instrument-coordinated (“XYZ”) velocities by using an instrument specific beam-to-xyz transformation matrix that defines each beam’s inclination and azimuth. Third, XYZ velocities are further converted to Earth-coordinated (“ENU”) velocities using the instrument’s physical orientation as taken by a heading and tilt sensor.

There are four interconnected considerations in the above process that have direct implication for surface buoy-mounted ADCPs:

1. Assumption of horizontal flow homogeneity (Fig. 1).
2. Timing gap between velocity and tilt sampling.

- Whether tilt measurements used in the XYZ-to-ENU conversion are applied at the ensemble level or for each individual ping.
- True tilt data is used to define exact position of each depth bin within the water column.

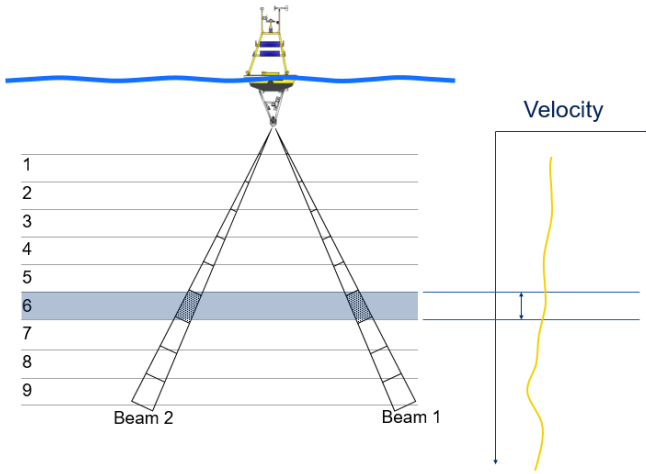


Fig. 1. ADCPs assume the flow to be homogenous across all its beams.

The first consideration is a rather safe and core assumption of all ADCPs: that the flow is homogenous across each depth bin over each measurement interval. This assumption almost always holds true for “normal” water bodies of interest and typical ADCP sampling durations. However, large ADCP tilts can lead to an artificial increase in each depth bin’s vertical extent causing a smearing of the velocity data, more pronounced with increasing range from the instrument (Fig. 2). This is further enhanced if strong vertical shear is present as the depth bins will constantly migrate into and out of regions with variable velocity.

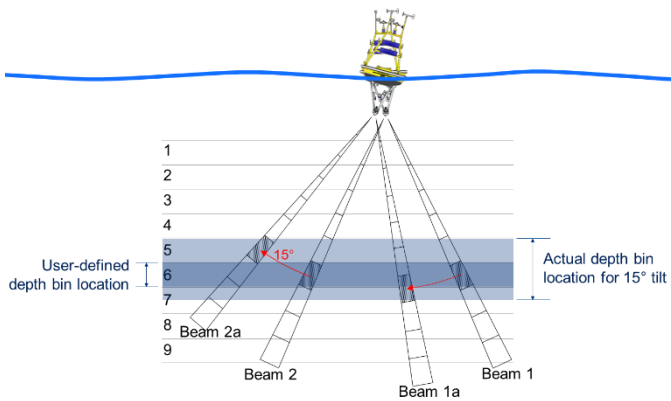


Fig. 2. When an ADCP is no longer perpendicular to the flow field, the vertical extent of each depth bin is artificially increased as a function of the tilt.

The second consideration defines the upper boundary for how much instrument motion can be accepted into the measurement before a significant impact to the measured velocity will occur. The greater the ADCP’s orientation rate of change within a measurement interval, the smaller the timing

gap needs to be between when the actual velocity estimate was performed and when the orientation was sampled. If the gap is too long, the position of each depth bins will be different than what is calculated based on the orientation measurement, with the difference increasing with range away from the instrument.

The third consideration is directly connected to the above. To reduce measurement uncertainty, an ADCP’s velocity profile is typically built into an ensemble which is the average of several individual pings. The conversion from XYZ to ENU factors in the instrument’s orientation as measured by its compass and tilt sensor. This conversion can be done at the ensemble level, or at the individual ping level. If done at the ensemble level, it is assumed that no instrument movement has occurred within the ensemble interval, which can last from a few seconds to several minutes and therefore quickly breakdown in dynamic conditions.

Finally, the fourth and most important consideration is that the orientation sensor used in the ADCP must be able to discern between accelerations due to gravity (that lead to tilt) and linear accelerations due to its own motion (that impart errors on the tilt); that is, it must be able to measure both static tilt as well as dynamic tilt. If not compensated, linear accelerations can cause significant errors in tilt (Fig.3), which then translate into velocity errors because the physical location of the depth bins is not at their user-defined location but rather are either above or below it.

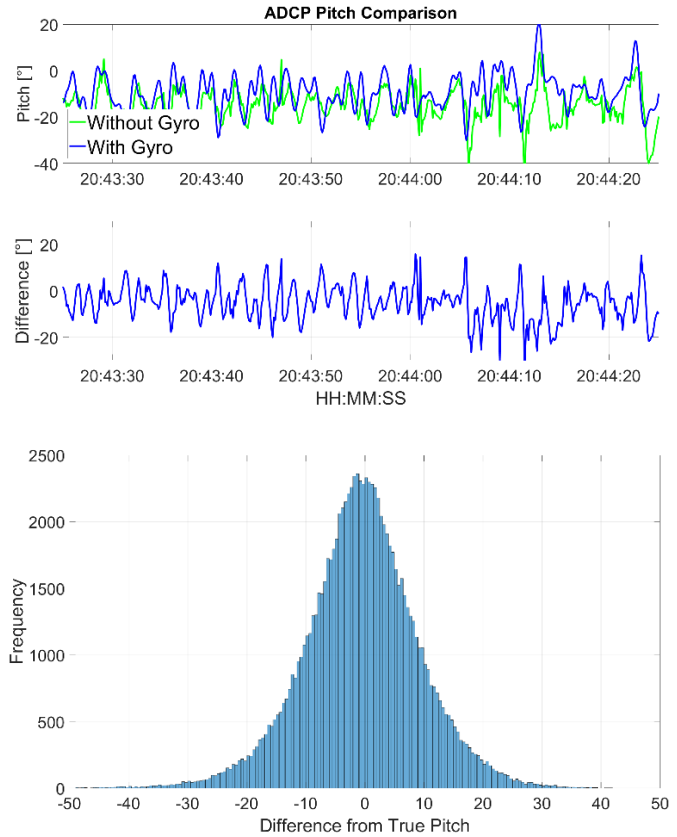


Fig. 3. Tilt (pitch) data recorded at 8 Hz from a Nortek Signature1000 ADCP mounted on a surface buoy. Wave conditions during this time were $H_s \sim 0.5$ m and $T_p \sim 4$ s. Top panel compares values computed from a standard 3-axis accelerometer tilt sensor with a gyro-compensated (true tilt) sensor.

Middle panel shows differences over the 60 s window. Bottom panel shows differences observed during the full 8-hour deployment. Errors in excess of $\pm 10^\circ$ are readily seen.

B. Static vs. Dynamic Tilt

Traditionally, ADCPs seldom needed dynamic tilt measurement. This was because they were either mounted on fixed (or slow moving) platforms, or when mounted on dynamically moving platforms such as vessels or surface buoys, the high frequency motion was filtered out of the data by long averaging intervals in space and/or time or via low-pass filters in post-processing. Today, however, with the increasing demand from the research and operational communities for ever finer spatial and temporal resolution, especially in the upper ocean and in mixing and advective processes research, averaging routines often used to compensate for the impact of motion in the velocity data are becoming less and less desirable. Alternatives are therefore warranted, especially for low-cost, low-power, and miniaturized solutions that can be embedded as part of the ADCP electronics.

Up to now, tilt sensors used in ADCPs have been based on 3-axis accelerometers which can only measure static tilt. These sensors are initialized at a known orientation and actually measure the acceleration of gravity along each axis off this initial orientation:

$$\theta = \arcsine(a_x) \quad (1)$$

$$\phi = \arctangent(-a_y, -a_z) \quad (2)$$

where θ is the pitch angle, ϕ is the roll angle, a_x , a_y , a_z are the accelerations due to gravity on each of the three axis. This can further be related to the ENU coordinate system through a transformation matrix, M :

$$M = \begin{bmatrix} \cos\theta & -\sin\theta\sin\phi & -\cos\phi\sin\theta \\ 0 & \cos\phi & -\sin\phi \\ \sin\theta & \sin\phi\cos\theta & \cos\theta\cos\phi \end{bmatrix} \quad (3)$$

The critical issue is that accelerometers respond not only to accelerations due to gravity, but also to linear accelerations. A simple analogy is demonstrated by rapidly sliding a glass of water along a flat tabletop—the surface of the water will tilt, even though the glass itself will not. In the case of an ADCP on a surface buoy, the wave-induced linear accelerations experienced by the buoy can cause significant errors in computed tilt as already shown in Fig. 3.

To address the limitation with tilt sensors based solely on accelerometer measurements, angular rate sensors (commonly called “gyros”) can be integrated with accelerometers to provide dynamic tilt measurements. This is possible because gyros respond only to rotational rate, and not to linear acceleration. Through the use of a Kalman filter, the combined 3-axis accelerometer plus 3-axis gyro provides a direct output of true tilt in dynamic conditions. This, further coupled with a 3-axis magnetometer can be packaged into a single sensor termed an Attitude and Heading Reference Sensor (AHRS) that provides dynamic tilt measurements.

C. Bin Mapping

Once true tilt can be measured, proper bin mapping can be done. This is the process of mapping the actual location of each depth bin, in BEAM coordinates, to their user-defined vertical position. This is conceptually illustrated in Fig. 4.

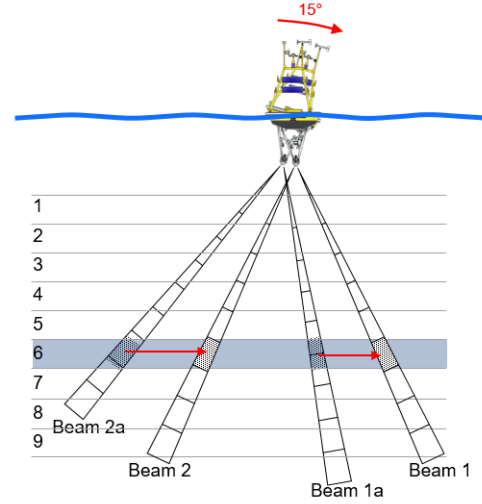


Fig. 4. When bin mapping is enabled, the location of each depth bin is shifted either up or down along each beam such that the resulting data comes from the proper user-defined depth, simulating a static system.

Although this method has been available in most ADCPs for over 20 years, it has so far been applied mostly at the ensemble level and the tilt has been measured by non-gyro-compensated tilt sensors capable of only measuring static tilt. But proper bin mapping has four main requirements, closely related to the four ADCP processing scheme considerations discussed earlier. First, the tilt data must be true dynamic tilt as measured by a gyro-compensated tilt sensor; otherwise, the incorrect orientation will be used and the resulting velocities affected. Second, the tilt sensor must be able to sample fast enough to capture the dynamic motions experienced by the ADCP. Third, the timing of the orientation sampling must be precisely synchronized with the velocity sampling (in the order of milliseconds) as any lag in this process will mean the wrong tilt is being applied. And fourth, the true tilt data must be applied to the velocity data on a ping-by-ping basis and not at the ensemble level, in order to correct the velocities at their most fundamental level.

Additionally, although not an absolute requirement, it is advantageous that the bin mapping routine be done in real-time. As one of the key advantages of a surface buoy-mounted ADCP is the easier access to real-time data for online applications, having the bin mapping done only at the post-processing level would be a limiting factor in most applications.

D. Implementation

To quantify the improvements proposed in this work, a Nortek Signature1000 ADCP (Fig. 5) was fully integrated with an internal high accuracy AHRS and mounted on surface buoy. The buoy was deployed near the mouth of the Chesapeake Bay, USA, which is a site known for strong tidal currents and

pronounced vertical shear. The deployment lasted from mid-December, 2017 to late January, 2018.

As expected of winter conditions in this region, the site observed a range of weather, from very calm to stormy conditions (Fig. 6). Velocity magnitude during the deployment ranged from ~ 0 m/s during slack tide to greater than 1.2 m/s driven by semidiurnal tides, often with pronounced vertical shear. Although shear in this area is often positive (top faster than bottom), there were several times when this situation was reversed.



Fig. 5. The Signature1000 is a 5-beam ADCP with optional embedded AHRS, 1000 kHz frequency and maximum sampling rate of 16 Hz.

The buoy was subjected to high degrees of tilt, in excess of 20° , in response to the wind and wave conditions. This was actually welcomed as it afforded several occasions during the deployment to test the proper real-time bin mapping algorithms. Additionally, the fact that the Signature1000 ADCP was mounted off-center on the buoy meant that at times of strong currents it acted as a rudder, minimizing rotation even though the higher frequency 8 Hz data from the AHRS (not shown) still indicates noticeable rotational rates during these times.

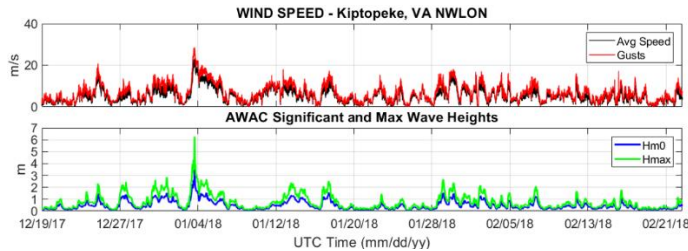


Fig. 6. Wind speed and gust during deployment duration at the site. During the storm on 04/Jan/2018, near surface water temperature was less than 1°C , as measured by the Signature1000's temperature sensor. It is believed the buoy was iced over during this time.

A Nortek AWAC 1 MHz ADCP was deployed as a reference system for this deployment. It was configured upward looking on a trawl resistant bottom mount, and installed around 190 m due north of the Signature1000 buoy. Both instruments set for 1 m depth bin sizes. For accurate comparison between the two systems, the dynamic Signature1000's bins were interpolated to the static AWAC bins as a function of the tide, such that direct comparisons between the two instruments can be made. The main Signature1000 configuration had it sampling 1200 pings at 8 Hz for 150 s every 360 s. Meanwhile, the AWAC was configured to measure currents for 120 s every 180 s and had a wave burst interweaved with currents for 2048 points at 1 Hz every hour. For further details about the location and each

instrument's configuration, the reader is referred to the previous work [1].

III. RESULTS AND DISCUSSION

Data from four selected periods are shown on Figs. 7-10. The four periods were chosen to represent the range of motions observed by the surface buoy and vertical shear during the deployment:

- High Shear, Low Acceleration; Fig. 7
 - 26/Jan/2018 08:55 – 26/Jan/2018 15:08
 - $H_{\text{mean}} \approx 0.1$ m and $T_{\text{mean}} \approx 3.5$ s
- Low Shear, Low Acceleration; Fig. 8
 - 22/Dec/2017 22:55 – 23/Dec/2017 07:01
 - $H_{\text{mean}} \approx 0.1$ m and $T_{\text{mean}} \approx 3.0$ s
- High Shear, High Acceleration; Fig. 9
 - 17/Jan/2018 14:20 – 17/Jan/2018 22:26
 - $H_{\text{mean}} \approx 0.7$ m and $T_{\text{mean}} \approx 3.8$ s
- Low Shear, High Acceleration; Fig. 10
 - 28/Dec/2017 08:30 – 28/Dec/2017 16:32
 - $H_{\text{mean}} \approx 0.8$ m and $T_{\text{mean}} \approx 4.0$ s

The data shown include depth-averaged velocity for both the reference system (AWAC) and the buoy-mounted Signature1000. The site is strongly aligned North-South, and so only the North component of the velocity is presented here, as it constitutes by far the dominant orientation. The AWAC was set to sample for both currents and directional waves, and so its data density during this deployment is not nearly as high as the Signature1000. At least four samples every hour overlapped, allowing for close computation of RMS Error (RMSE) for several samples. Current profiles from the AWAC were also used to compute vertical shear, defined here as the difference from the top 1/3 of the water column and the bottom 1/3, and shown in Figs. 7-10 as absolute values. Finally, utilizing the 3-axis accelerometer component of the AHRS inside the Signature1000, the acceleration magnitude experienced by the buoy is shown. Here the acceleration due to gravity (1 g) has been removed to highlight the variability from steady state.

Fig. 7 illustrates a very calm surface condition where the buoy's acceleration was at a minimal. In fact, this was the time chosen to retrieve the buoy due to the calm condition and the buoy's removal from the water can be seen by a sudden increase in acceleration at the very end of the data set (around 15:10). Shear during this period is moderate and variable, reaching up to about 40 cm/s just prior to the buoy's retrieval. The RMSE of the Signature1000 North Velocity is less than 3 cm/s under these conditions.

Fig. 8 represents a time when the buoy's acceleration went through a transition between two wave events, with shear starting moderately at about 20 cm/s but the quickly diminishing as the water column became more mixed. Similarly, almost all of the RMSE values are less than 3 cm/s.

A storm event around 17/Jan/2018 brought bigger waves, with $H_{\text{max}} > 2$ m at times. During this time, the buoy observed strong acceleration of almost ± 1 g, while the water column experienced strong shear gradient of greater than 50 cm/s difference from top to bottom (Fig. 9). Consequently, the difference from the bottom-mounted reference AWAC and the

buoy-mounted Signature1000 increased noticeably. However, due to the proper compensation from the AHRS, the RMSE stayed under 10 cm/s for most of the event.

Fig. 10 shows another period of high acceleration and with relatively low shear. As most of the surface buoy's acceleration is derived from waves and wind, and these tend to mix the water

column, the conditions illustrated on this period were common during the deployment. Variability with the reference system remained relatively low, however, with RMSE values seldom exceeding 5 cm/s.

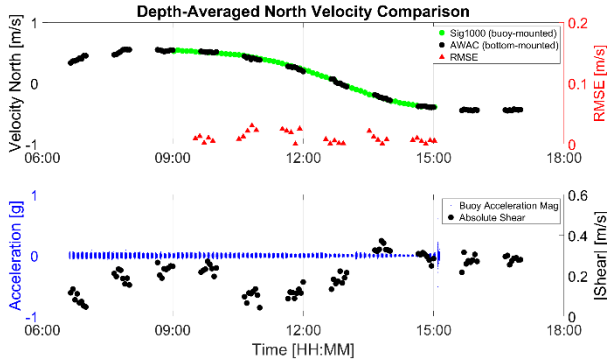


Fig. 7. Time period with high shear and low buoy acceleration.

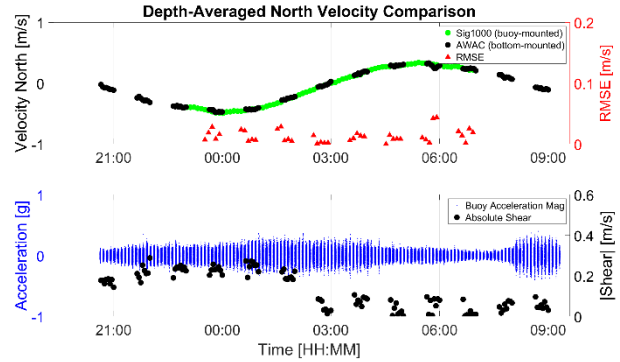


Fig. 8. Time period with moderate to low shear and moderate to low buoy acceleration.

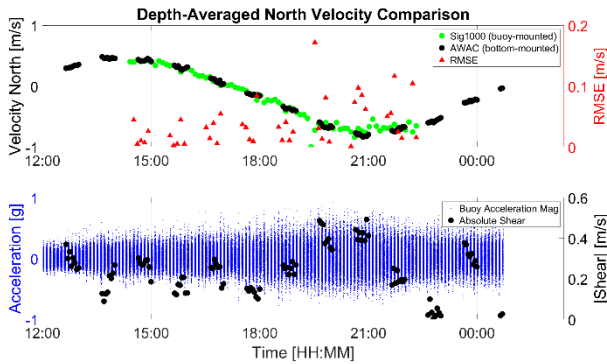


Fig. 9. Time period with high shear and high buoy acceleration.

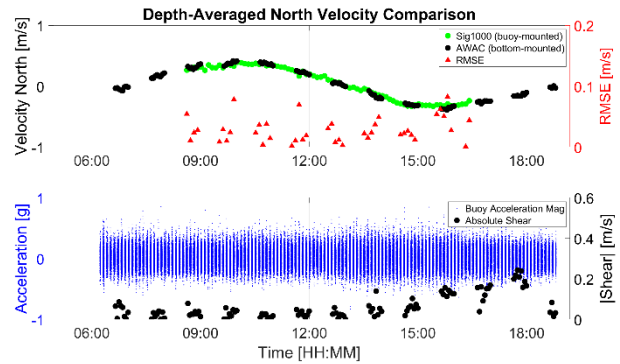


Fig. 10. Time period with low shear and high buoy acceleration.

The level of accuracy shown in these data is significant, especially when considering the high dynamic condition that the Signature1000 was subjected to during most of this deployment. The comparisons shown are typical of two fixed, bottom-mounted ADCPs, yet the proper integration of an AHRS onto the Signature1000 has allowed for a surface-buoy mounted system to be made equivalent to a bottom-mounted ADCP.

Another benefit of the AHRS is the fact that the data from each of its three separate sensors (accelerometer, magnetometer and angular rate sensor) are independently recorded by the Signature1000 at the same ping rate as the velocity. This allows for reprocessing the tilt data without the angular rate (gyro) data, thus simulating what a "standard" tilt sensor would behave like in the exact same condition. Normally, most ADCP tilt sensors have a response rate typically no better than 1 Hz, so in order to make a proper comparison, the data was also subsampled down to 1 Hz in addition to having the tilt be computed with just the accelerometer data as it is done with a standard tilt sensor. Sample results are illustrated in Fig. 11, where the same time

period shown on Fig. 9 (17/Jan/2018 14:20 – 22:26) was selected and the velocity re-processed in two ways: 1) simulating a standard tilt sensor and performing bin-mapping with this tilt (top panel), and 2) simulating a standard tilt sensor but doing no bin-mapping (bottom panel). It clearly shows how the full AHRS compensated velocity data (Fig. 9) is a closer match to the reference AWAC, but also highlights the level of error that can be introduced in a current profile computed without a gyro-compensated tilt sensor.

Furthermore, the impact of vertical shear is also illustrated. When shear increases right after slack water (after about 18:00), the error between the bottom-mounted reference system and buoy-mounted system increases significantly, reaching values almost as high as the velocity itself (i.e. almost 100% difference). In comparison, the same data as shown in Fig. 9, where the true dynamic tilt was used in the velocity computation, shows a great agreement between the bottom-mounted reference and buoy-mounted system, even during high acceleration and high shear conditions.

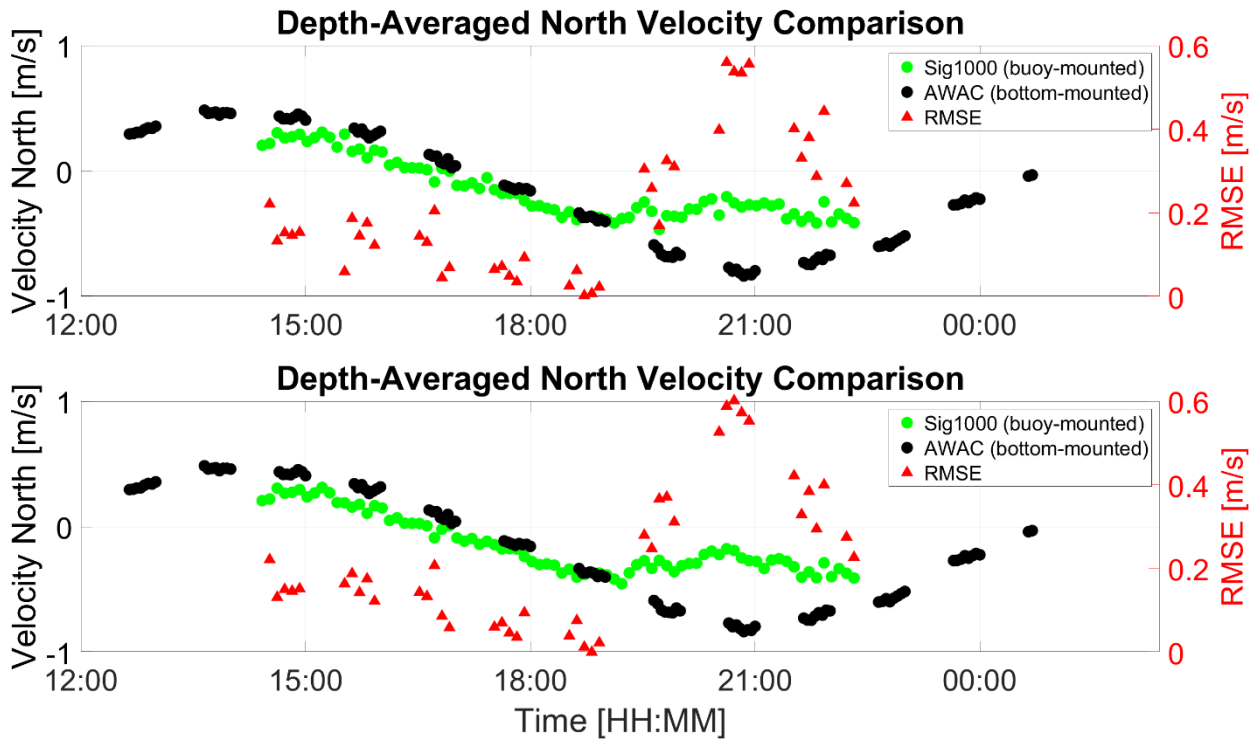


Fig. 11. Comparison of velocity re-processed with standard tilt. Top panel is velocity processed with standard tilt and also bin-mapped. Bottom panel is velocity processed with standard tilt but not bin mapped. Data from same time period as Fig. 9. Note change of RMSE scale as compared to Fig. 9 as difference between buoy-mounted sensor and bottom-mounted reference are much higher when velocity is processed as just a standard tilt sensor.

IV. CONCLUSIONS

The benefits of installing ADCPs on surface buoys are significant. However, several previous work have shown that surface buoy-mounted ADCP current profile data can be negatively impacted by buoy motion. In this work we have shown how the advantages that an Attitude and Heading Reference Sensor (AHRS) can bring to current profile data collected from surface buoys. The AHRS's capability to

measure dynamic tilt, rather than just standard tilt as is effectively always done with ADCPs, helps to improve data accuracy and opens up opportunities to install ADCPs where previously no possible.

V. ACKNOWLEDGEMENTS

The authors would like to thank the staff of the NOAA CO-OPS office in Chesapeake, VA, USA, for all the assistance in deploying and recovering the buoy used in this study.

VI. REFERENCES

- [1] D. W. Velasco, W. D. Wilson, S. Nylund and R. Heitsenrether, "Enhancing the Accuracy of Current Profiles from Surface Buoy-Mounted Systems," 2018 OCEANS - MTS/IEEE Kobe Techno-Oceans (OTO), Kobe, 2018, pp. 1-6.
- [2] A. J. Plueddemann, R. A. Weller, T. D. Dickey, J. Marra, G. H. Tupper, B. S. Way, W. M. Ostrom, P. R. Bouchard, A. L. Oien, N. R. Galbraith, "The Marine Light-Mixed Layer Experiment Cruise and Data Report, R/V Endeavor, Cruise EN-224, Mooring Deployment, 27 April-1 May 1991, Cruise EN-227, Mooring Recovery, 5-23 September 1991," Upper Ocean Processes Group, Woods Hole Oceanogr. Inst., Woods Hole, MA, USA, Tech. Rep. WHOI-93-33, 1993.
- [3] F. Schott, W. Johns, "Half-year-long measurements with a buoy-mounted acoustic Doppler current profiler in the Somali current," *J. Geoph. Res.*, vol. 92, pp. 5169-5176, 1987.
- [4] N. R. Pettigrew, J. D. Wood, E. H. Pape, G. J. Needell, J. D. Irish, "Acoustic Doppler current profiling from moored subsurface floats," in *Oceans '87, Proceedings*. Halifax, NS, Canada, pp. 110-116, 1987.
- [5] C. A. Alessi, S. J. Lentz, R. C. Beardsley, "Shelf mixed layer experiment (SMILE) program description and coastal and moored array data report," Dept. Phys. Oceanogr., Woods Hole Oceanogr. Inst., Woods Hole, MA, USA, Tech. Rep. WHOI-91-39, 1991.
- [6] J. D. Irish, K. E. Morey, N. R. Pettigrew, "Solar-powered, temperature/conductivity/Doppler profiler moorings for coastal water with ARGOS positioning and GOES telemetry," in *Oceans '92, Proceedings*. Newport, RI, USA, pp. 730-735, 1992.
- [7] R. Weisberg, B. Black, I. C. Donovan, R. Cole, "The west-central Florida shelf hydrography and circulation study: a report on data collected using a surface moored acoustic Doppler current profiler, October 1993-January 1995," Dept. Mar. Sci., Univ. South Florida, St. Petersburg, FL, USA, pp. 127.
- [8] P. E. Pullen, M. J. McPhaden, H. P. Freitag, J. Gast, "Surface wave induced skew errors in acoustic Doppler current profiler measurements from high shear regions," in *Oceans '92, Proceedings*. Newport, RI, USA, pp. 706-711, 1992.
- [9] P. E. Plimpton, H. P. Freitag, M. J. McPhaden, "ADCP Velocity Errors from Pelagic Fish Schooling around Equatorial Moorings," *J. Atmos. Oceanic Tech.*, vol. 14, pp. 1212-1223, 1997.
- [10] C. Winant, T. Mettlach, S. Larson, "Comparison of buoy-mounted 75-kHz acoustic Doppler current profilers with vector-measuring current meters," *J. Atmos. Oceanic Tech.*, vol. 11, pp. 1317-1333, 1994.

- [11] A. Lohrmann, "Comparison of buoy mounted NDP current velocity data with upward looking ADCP data," Nortek AS, Oslo, Norway, Tech. Note 001, 1998.
- [12] D. Mayer, J. Virmani, R. Weisberg, "Velocity comparisons from upward and downward acoustic Doppler current profilers on the West Florida shelf," *J. Atmos. Oceanic Tech.*, vol. 24, pp. 1950-1960, 2007.
- [13] H. Seim, C. Edwards, "Comparison of buoy-mounted and bottom-moored ADCP performance at Gray's Reef," *J. Atmos. Oceanic Tech.*, vol. 24, pp. 270-284, 2007.
- [14] K. Bosley, C. McGrath, J. Dussault, M. Bushnell, M. Evans, G. French, K. Earwaker, "Test, evaluation, and implementation of current measurement systems on aids-to-navigation," Center Oper. Oceanogr. Products and Services, Natl. Ocean. Atmos. Admin., Silver Spring, MD, USA, Tech. Rep. NOS CO-OPS 043, 2005.
- [15] R. Kashino, T. Ethier, R. Phillips, "TRIAxYS acoustic Doppler current profiler comparison study," Axys Technologies, Sidney, BC, Canada, pp. 21.
- [16] L. K. Locke, R. Crout, "A study on the validity of buoy mounted acoustic Doppler profilers: a comparison of upward and downward looking systems in Onslow Bay, NC," in *Oceans 2009*. Biloxi, MS, USA, 2009.
- [17] W. D. Wilson, E. Siegel, "Evaluation of current and wave measurements from a coastal buoy," in *Oceans 2008*. Quebec City, QC, Canada, 2008.
- [18] W. D. Wilson, E. Siegel, "Current and wave measurements in support of the Chesapeake Bay Interpretive Buoy System," in *Tenth Working Conference on Current Measurement Technology*. Monterey, CA, USA, 2010.
- [19] R. Heitsenrether, N. Holcomb, G. Gray, C. C. Teng, W. D. Wilson, "NOAA's recent field testing of current and wave measurement systems – part I," in *Eleventh Working Conference on Currents, Waves and Turbulence Measurement*. St. Petersburg, FL, USA, 2015.
- [20] W. D. Wilson, R. Heitsenrether, G. Gray, N. Holcomb, C. C. Teng, "NOAA's recent field testing of current and wave measurement systems – part II," in *Eleventh Working Conference on Currents, Waves and Turbulence Measurement*. St. Petersburg, FL, USA, 2015.
- [21] W. D. Wilson, R. Heitsenrether, N. Holcomb, "A comparison of current profiles collected from bottom- and buoy-mounted instruments," in *Oceans 2016*. Monterey, CA, USA, 2016.
- [22] D. Shumuk, B. Michael, D. Velasco and W. Douglas Wilson, "The Next Generation of Buoys Integrated with Current Profilers," *OCEANS 2018 MTS/IEEE Charleston*, Charleston, SC, 2018, pp. 1-6.